

Can pre-ozonation be combined with gravity-driven membrane filtration to treat shale gas wastewater?

*Original*

Can pre-ozonation be combined with gravity-driven membrane filtration to treat shale gas wastewater? / Tang, Peng; Shi, Mengchao; Li, Xin; Zhang, Yongli; Lin, Dong; Li, Tong; Zhang, Weiming; Tiraferri, Alberto; Liu, Baicang. - In: SCIENCE OF THE TOTAL ENVIRONMENT. - ISSN 0048-9697. - 797:(2021), p. 149181.  
[10.1016/j.scitotenv.2021.149181]

*Availability:*

This version is available at: 11583/2915978 since: 2021-07-30T11:18:15Z

*Publisher:*

Elsevier B.V.

*Published*

DOI:10.1016/j.scitotenv.2021.149181

*Terms of use:*

This article is made available under terms and conditions as specified in the corresponding bibliographic description in the repository

*Publisher copyright*

(Article begins on next page)

1 Can pre-ozonation be combined with gravity  
2 driven membrane filtration to treat shale gas  
3 wastewater?

4 *Peng Tang*<sup>a,b</sup>, *Mengchao Shi*<sup>a,b</sup>, *Xin Li*<sup>a,b</sup>, *Yongli Zhang*<sup>a</sup>, *Dong Lin*<sup>c</sup>, *Tong Li*  
5 *d,\**, *Weiming Zhang*<sup>e</sup>, *Alberto Tiraferri*<sup>f</sup>, *Baicang Liu*<sup>a,b,\*\*</sup>

6 <sup>a</sup> Key Laboratory of Deep Earth Science and Engineering (Ministry of Education),  
7 College of Architecture and Environment, Institute of New Energy and Low-Carbon  
8 Technology, Institute for Disaster Management and Reconstruction, Sichuan University,  
9 Chengdu, Sichuan 610207, PR China

10 <sup>b</sup> Yibin Institute of Industrial Technology, Sichuan University, Yibin Park, Section 2,  
11 Lingang Ave., Cuiping District, Yibin, Sichuan 644000, PR China

12 <sup>c</sup> PetroChina Southwest Oil and Gas field Company, No.5 Fuqing Rd., Chengdu,  
13 Sichuan 610051, PR China

14 <sup>d</sup> School of Energy and Environmental Engineering, University of Science &  
15 Technology Beijing, Beijing, 100083, PR China

16 <sup>e</sup> State Key Laboratory of Pollution Control and Resource Reuse, School of the  
17 Environment, Nanjing University, Nanjing 210023, PR China

18 <sup>f</sup> Department of Environment, Land and Infrastructure Engineering, Politecnico di  
19 Torino, Corso Duca degli Abruzzi 24, 10129 Turin, Italy

20

21 **Abstract:** Low-cost gravity-driven membrane (GDM) filtration combined with  
22 appropriate pre-treatment processes has major potential to efficiently manage shale  
23 gas wastewater (SGW). In this work, the feasibility of combining low dosage  
24 pre-ozonation with the GDM process was evaluated in the treatment of SGW. The  
25 results showed that pre-ozonation significantly increased the stable flux (372%) of  
26 GDM filtration, while slightly deteriorating the quality of the effluent water in terms  
27 of organic content (-14%). These results were mainly attributed to the conversion of  
28 macromolecular organics to low-molecular weight fractions by pre-ozonation.  
29 Interestingly, pre-ozonation markedly increased the flux (198%) in the first month of  
30 operation also for a GDM process that comprised the addition of GAC (GGDM).  
31 Nevertheless, the flux of O<sub>3</sub>-GGDM systems dropped sharply around the 25th day of  
32 operation, which might be due to the rapid accumulation of pollutants in the high flux  
33 stage and the formation of a dense fouling layer. Pre-ozonation remarkably influenced  
34 the microbial community structure and O<sub>3</sub>-GDM systems were characterized by  
35 distinct core microorganisms, which could degrade specific organics in SGW.  
36 Furthermore, O<sub>3</sub>-GDM outperformed simple GDM as a pretreatment for RO. These  
37 findings can provide valuable references for combining oxidation technologies with  
38 the GDM process in treating refractory wastewater.

39

40 **Keywords:** Shale gas wastewater; Pre-ozonation; Gravity driven membrane filtration;  
41 Mechanism

## 42 **1. Introduction**

43 Horizontal drilling and hydraulic fracturing technologies are applied to overcome  
44 the challenge of shale gas extraction. Nevertheless, a large amount (~5200-25,870 m<sup>3</sup>  
45 per well) of shale gas wastewater (SGW) is produced during hydraulic fracturing  
46 (Kondash and Vengosh, 2015). SGW is typically characterized by high salinity and  
47 high concentrations of toxic metals and organics (Butkovskyi et al., 2017). If not  
48 treated properly, its discharge would seriously threaten the water environment and  
49 human health. At present, hybrid membrane technologies are regarded as suitable and  
50 effective means to treat SGW (Tong et al., 2019). Specifically, low-pressure  
51 membrane processes, such as ultrafiltration (UF), are investigated and implemented as  
52 pretreatment steps for the subsequent desalination (Chang et al., 2019b; Guo et al.,  
53 2018; Miller et al., 2013). However, operational problems associated with membrane  
54 fouling seriously reduce the efficacy and economy of UF (Shang et al., 2019; Tang  
55 et al., 2020).

56 Gravity driven membrane filtration (GDM), a recently developed membrane  
57 technology, has been proposed to replace traditional UF in the pretreatment of SGW  
58 (Chang et al., 2019a). The main rationale is that GDM filtration does not need  
59 cleaning and can obtain a stable flux driven solely by gravity with the advantages of  
60 simple operation, low cost, and low energy consumption (Pronk et al., 2019). The  
61 feasibility of the GDM process as a pretreatment option for SGW desalination was  
62 verified in a number of research efforts (Chang et al., 2019a; Tang et al., 2021a).

63 While underlining the potential of GDM filtration, these studies highlighted the  
64 current need for significant improvements in stable flux values and contaminant  
65 removal rates of this technology (Chang et al., 2019a; Tang et al., 2021a).

66 Some processes, including adsorption, aeration, and coagulation were  
67 successfully combined with GDM to the purpose of improving its performance (Ding  
68 et al., 2016; Lee et al., 2021; Tang et al., 2021c). As a strong oxidant, ozone was  
69 shown to effectively alleviate membrane fouling when used as a pretreatment process  
70 for UF and for membrane bioreactors (MBR) (Sathya et al., 2019; Tang et al., 2020;  
71 Wang et al., 2017; Zhang et al., 2020), owing to a reduction of organics molecular  
72 size, an enhancement of foulants hydrophilicity, and a decrease of biofouling (Wang  
73 et al., 2017). Therefore, we hypothesize that pre-ozonation should also effectively  
74 increase the performance of GDM filtration. Generally, it is not recommended to  
75 combine pre-ozonation with GDM in the treatment of drinking water, because  
76 pre-ozonation has the risk of deteriorating water quality and may produce toxic  
77 by-products (Tang et al., 2021b). On the other hand, these issues should not impact  
78 the application of GDM filtration to treat wastewater, because this technology would  
79 not act as a final polishing step, but instead as pretreatment for subsequent tertiary or  
80 desalination processes. The high potential of applying advanced oxidation in the  
81 specific treatment of SWG and other producted waters has been recently highlighted  
82 and it is of great significance to study synergy of ozonation and GDM filtration, two  
83 of the most promising processes for efficient SGW management.

84 Therefore, in this study pre-ozonation is investigated in combination with GDM  
85 filtration to treat SGW with the aim of increasing stable flux and contaminant removal  
86 values in GDM, and improving the quality of the final desalinated effluent. Six GDM  
87 systems are examined to understand the effect of pre-ozonation with low ozone  
88 dosage on the performance of GDM systems with and without the presence of an  
89 additional treatment step through activated carbon adsorption. The integration  
90 between pre-ozonation and GDM filtration is thus discussed, also in the light of the  
91 effect on microbial communities that drive membrane fouling and organics removal  
92 and biodegradation within the GDM unit.

93

## 94 **2. Materials and methods**

### 95 **2.1 Water samples and water quality analysis**

96 SGW samples were collected from the Weiyuan shale gas play (Sichuan Basin,  
97 China). The water quality parameters of the SGW are summarized in [Table 1](#). The  
98 analytical methods for the determination of turbidity, dissolved organic carbon (DOC),  
99 UV<sub>254</sub>, fluorescent organics, and total dissolved solid (TDS) can be found in [Text S1](#)  
100 of the Supporting Information (SI) and in our previous study (Tang et al., 2020).

101 **Table 1.** Water quality characteristics of the raw water and the raw water treated by O<sub>3</sub>  
102 at different dosages.

Parameter	Raw water	Raw water treated by O <sub>3</sub>		
		20 mg/L	40 mg/L	80 mg/L
DOC (mg/L)	17.48	17.91	18.95	18.54

UV <sub>254</sub> (cm <sup>-1</sup> )	0.095	0.097	0.100	0.098
Turbidity (NTU)	8.2	7.7	7.2	9.6
TDS (g/L)	19.85	20.14	20.71	19.86

## 103 2.2 Experimental setups and procedures

104 The schematic diagrams and the parameters of the six GDM systems utilized in  
105 this work are shown in Fig. S1 and Table 2, respectively. The systems were operated in  
106 parallel at room temperature (10-26 °C, Fig. S2) with a hydrostatic pressure of 70 mbar  
107 as driving force. The characteristics of the poly(vinylidene fluoride) hollow fiber UF  
108 membranes (Litree Purifying Technology Co., Ltd., China) with an effective membrane  
109 area of 10 cm<sup>2</sup> employed in this study can be found in a previous report (Chang et al.,  
110 2019a). The systems ran continuously for 90 days, and the flux was monitored  
111 through the electronic balance.

112 The system referred to as GDM1 treated raw water without any pre-treatment  
113 and represented the control unit. On the other hand, the feed water of four of the six  
114 GDM systems (namely, GDM-3, 4, 5, 6) was raw water treated by O<sub>3</sub> at different  
115 dosages. Low ozone dosages (20-80 mg/L) were applied and the detailed description  
116 of the pre-ozonation process can be found in our previous work (Tang et al., 2020).  
117 Before the subsequent GDM filtration, the residual ozone in water was quenched by  
118 heating the ozonated effluent at 50 °C for 30 min.

119 Granular activated carbon (GAC, CPG LF 12, Calgon Carbon Co., Ltd., USA)  
120 adsorption was included in four of the six GDM systems, specifically, GDM-2, 3, 5, 6.  
121 The four systems comprising adsorption are referred to as GGDM units. The GAC

122 was cleaned with deionized water and dried before use. A dosage of 4 g was used to  
 123 pre-treat the influent water to the GDM system, a much smaller quantity than that  
 124 used in our previous study (Tang et al., 2021a), to slightly reduce the adsorption effect  
 125 and highlight the effect of microbial degradation in the membrane reactor.

126 Reverse osmosis (RO) filtration experiments were carried out to verify the effect  
 127 of different GDM pre-treatment systems on the desalination performance. The RO  
 128 process was operated at a constant applied pressure of 5.5 MPa (55 bar) with 50%  
 129 recovery. The RO setup and membrane are described in detail in our previous work  
 130 (Tang et al., 2020).

131 **Table 2.** The parameters of six GDM systems.

No.	Aeration	The addition of GAC	Pre-ozonation
GDM1 (GDM)	10 ml/min	-	-
GDM2 (GGDM)	10 ml/min	4 g	-
GDM3 (O <sub>3</sub> <sup>20</sup> -GGDM)	10 ml/min	4 g	20 mg/L O <sub>3</sub>
GDM4 (O <sub>3</sub> <sup>40</sup> -GDM)	10 ml/min	-	40 mg/L O <sub>3</sub>
GDM5 (O <sub>3</sub> <sup>40</sup> -GGDM)	10 ml/min	4 g	40 mg/L O <sub>3</sub>
GDM6 (O <sub>3</sub> <sup>80</sup> -GGDM)	10 ml/min	4 g	80 mg/L O <sub>3</sub>

### 132 2.3 Analysis of the membrane fouling layers

133 The measurement and calculation methods of hydraulic resistance of the  
 134 membrane fouling layers, namely, the reversible resistance ( $R_{re}$ ) and the irreversible  
 135 resistance ( $R_{ir}$ ), were identical to our previous study (Chang et al., 2019a). The pure  
 136 water contact angles and Fourier transform infrared (FTIR) spectra of membrane  
 137 fouling layers were measured with a KRÜSS DSA 25S instrument (KRÜSS GmbH,  
 138 Germany) and with an attenuated total reflectance FTIR spectrometer (Nicolet IS 20,



139 Thermo Fisher Scientific Inc., USA), respectively. The surface and the cross-section  
140 of the fouled membrane samples, as well as the thickness of membrane fouling layers,  
141 were observed and measured by scanning electron microscopy (SEM) (FE-SEM,  
142 Regulus-8230, Hitachi, Japan). The surface roughness of the fouled UF membrane  
143 samples was determined with atomic force microscopy (AFM, Icon, Bruker,  
144 Germany). The extracellular polymer substances (EPS) extraction was conducted  
145 using a heating and sonication method and the EPS measuring protocol can be found  
146 in our recent studies (Tang et al., 2021d). The fluorescent compounds comprised in  
147 the EPS matrix were measured by fluorescence excitation-emission (EEM) (F7000,  
148 Hitachi, Japan)

#### 149 **2.4 Microbial diversity analysis**

150 The variation of the microbial community and the dominant functional  
151 microorganisms were analyzed through microbial diversity sequencing of the raw  
152 water and membrane fouling layers. The amplified primer sets of 16S rRNA genes for  
153 bacteria was 338F/806R. Details about microbial diversity sequencing and analysis  
154 are presented in [Text S2](#) of the SI and in our previous study (Tang et al., 2021a).

### 155 **3. Results and discussion**

#### 156 **3.1 Permeate flux and organic matter removal performance**

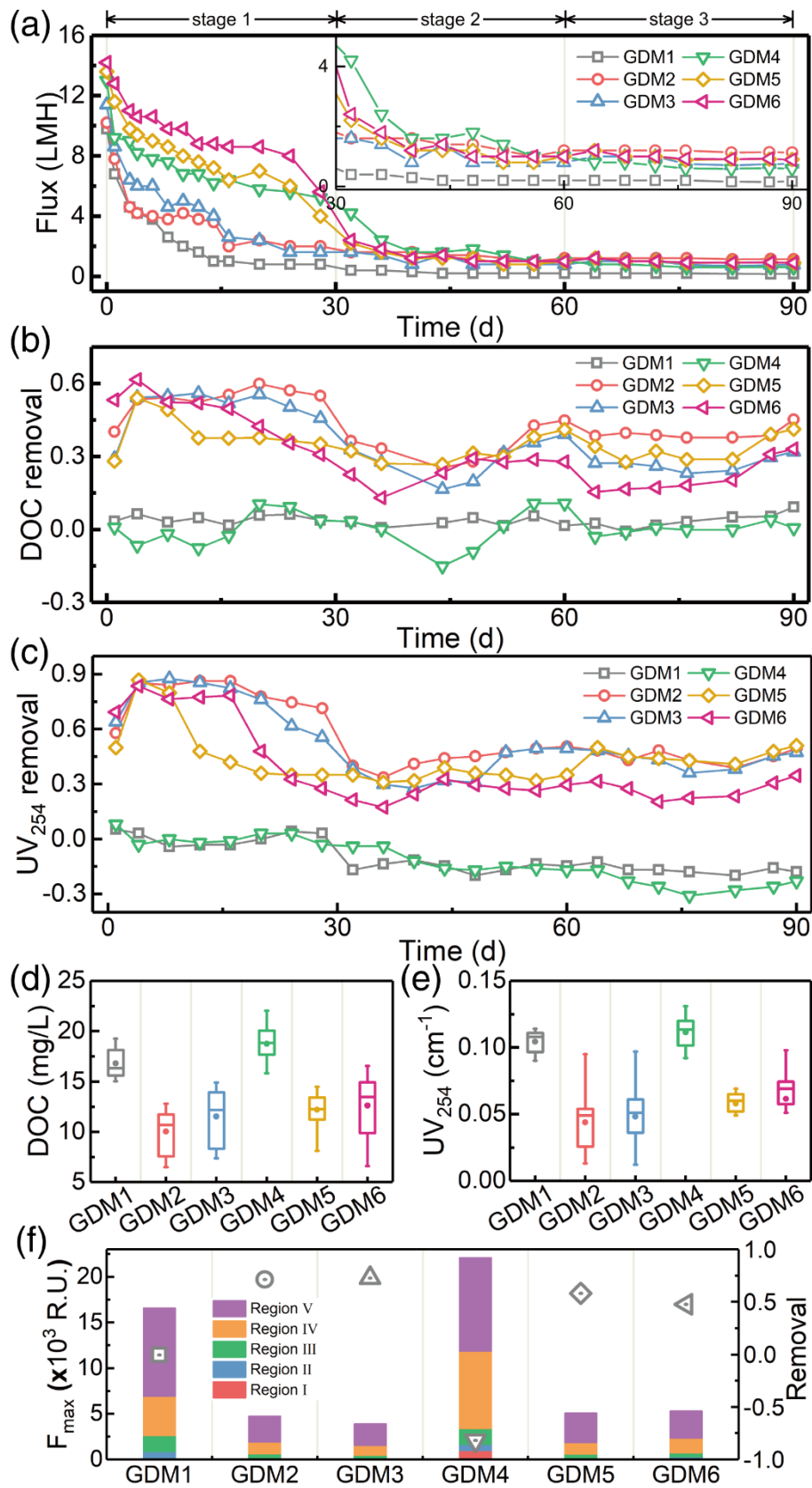
157 The hypothesis of this study is that pre-ozonation performance should influence  
158 the behavior of the subsequent GDM filtrations, with possibly higher productivity  
159 achievable in the membrane step. As presented in [Table 1](#), the DOC and UV<sub>254</sub>

160 parameters in the raw stream did not decrease upon oxidation, most likely due to the  
161 competing effect of mineralization and solubilization of organics (Tang et al., 2021b).  
162 Our previous research showed that pre-ozonation mainly changed the organic  
163 composition and characteristics of SGW, rather than translating into mineralization of  
164 compounds (Tang et al., 2020; Tang et al., 2021b). For example, pre-oxidation  
165 significantly improved the biodegradability of SGW (Liu et al., 2018; Tang et al.,  
166 2020). The composition and relative content of fluorescent organic matter components  
167 in SGW are shown in Fig. S3. The soluble microbial by-product-like matters (region  
168 IV) and humic acid-like matters (region V) were the dominant fluorescent organic  
169 components in SGW: 3.1%-38.6% of fluorescent organic components were removed  
170 by O<sub>3</sub>.

171 The flux profiles measured in the six GDM systems are presented in Fig. 1a and  
172 analyzed in the light of the pre-oxidation results. The flux trends can be divided into  
173 three stages. During the initial filtration stage (stage 1, 0-30 days), a monotonic  
174 decline of flux occurred in all the units. However, the flux of GDM systems treating  
175 pre-ozonized SGW dropped very slowly and was significantly higher than that of the  
176 control GDM system and of the GGDM system without pre-oxidation (GDM2).  
177 Specifically, the average flux in the O<sub>3</sub><sup>40</sup>-GDM system was 2.8 times that of GDM  
178 and 2.0 times that of GGDM. This result may be attributed to the degradation of  
179 macromolecular organic compounds by O<sub>3</sub> into low molecular-weight and more  
180 hydrophilic molecules that take more time to deposit on the membrane surface (Tang

181 et al., 2020). However, on the 25th day of operation, the fluxes of O<sub>3</sub>-GDM systems  
182 also dropped sharply and this phenomenon may be due to the rapid accumulation of  
183 pollutants due to the relatively high flux upon the formation of a more homogeneous  
184 coating layer at this point of the experiment.

185 Later, the fluxes in the systems continually decreased (second stage, 30-60 days),  
186 and ultimately tended to converge to roughly the same steady value (third stage, 60-90  
187 days), due to the formation of stable fouling layers on the membrane surfaces. The  
188 final stable flux values in the GDM, GGDM, O<sub>3</sub><sup>20</sup>-GGDM, O<sub>3</sub><sup>40</sup>-GDM, O<sub>3</sub><sup>40</sup>-GGDM,  
189 and O<sub>3</sub><sup>80</sup>-GGDM units were 0.18, 1.17, 0.85, 0.67, 0.97, and 0.98 L m<sup>-2</sup>h<sup>-1</sup> (LMH),  
190 respectively. These results suggest that pre-treatment significantly increased the  
191 productivity of the GDM filtration and that: (i) the productivity increased non-linearly  
192 but monotonically with ozone dosage; (ii) GAC adsorption significantly helped  
193 increasing the GDM flux.



194

195 Fig. 1. (a) Flux profile; (b) DOC removal; and (c) UV<sub>254</sub> removal measured in the six

196 GDM systems. Values of (d) DOC, (e) UV<sub>254</sub> in the six effluents. (f) Removal rate and

197 content of fluorescent organics in the effluent of the six systems. GDM1, GDM2,  
198 GDM3, GDM4, GDM5, and GDM6 represent control GDM, GGDM, O<sub>3</sub><sup>20</sup>-GGDM,  
199 O<sub>3</sub><sup>40</sup>-GDM, O<sub>3</sub><sup>40</sup>-GGDM, and O<sub>3</sub><sup>80</sup>-GGDM units, respectively.

200

201 [Fig. 1b](#) and [Fig. 1c](#) present the variation of DOC removal and UV<sub>254</sub> removal  
202 rates in the six GDM systems. This rate decreased firstly, then increased, and gradually  
203 stabilized. The gradual decrease of GAC adsorption sites is considered to be the main  
204 reason for the decline of removal rate in the initial stage; note that the two systems that  
205 did not comprise an adsorption process had near zero organics removal in the beginin of  
206 the experiments. On the other hand, the increase in removal rate in the second part of  
207 the tests may be attributed to the enhancement of microbial degradation and the  
208 formation of denser membrane fouling layers (Tang et al., 2021c; Tang et al., 2021d).  
209 Instead, the control GDM system and the O<sub>3</sub><sup>40</sup>-GDM system (no GAC adsorption)  
210 showed no or decreasing removal rates of organics components, which reached  
211 netagive values for UV<sub>254</sub> compounds.

212 Overall, these observations also support the conclusion that O<sub>3</sub> degraded  
213 macromolecular organics into low molecular weight fractions which, when not  
214 pre-adsorbed, could directly and more easily pass through into the permeate or  
215 undergo biodegradation within the fouling layers, thus further enhancing the passage  
216 through the membrane pores. [Fig. 1f](#) presents the composition and the relative content  
217 of fluorescent organic compounds in the effluent of the six GDM systems. The four

218 GGDM systems were associated with fluorescent organic compounds (47.6-72.8%).  
219 However, the removal rate of fluorescent organic compounds, indicative of soluble  
220 microbial by-product-like matters, was negative in the O<sub>3</sub><sup>40</sup>-GDM system. A factor  
221 that should also be considered when analyzing removal results is the phenomenon of  
222 concentration (Tang et al., 2021a). Since our GDM systems were based on dead-end  
223 filtration, contaminants would be concentrated in the reactor and this concentration  
224 would be more important for systems associated with higher flux values. We assessed  
225 the DOC value in the GDM reactors. (Fig. 1d and Fig. 1e): adsorption effectively  
226 reduced the amount of organics in the feed streams to the membranes, and this  
227 amount was the highest in the O<sub>3</sub><sup>40</sup>-GDM system, thus also contributing to a more  
228 challenging separation and overall negative values of organics removal. Not  
229 surprisingly, the higher the productivity of the systems the larger was the observed  
230 DOC concentration.

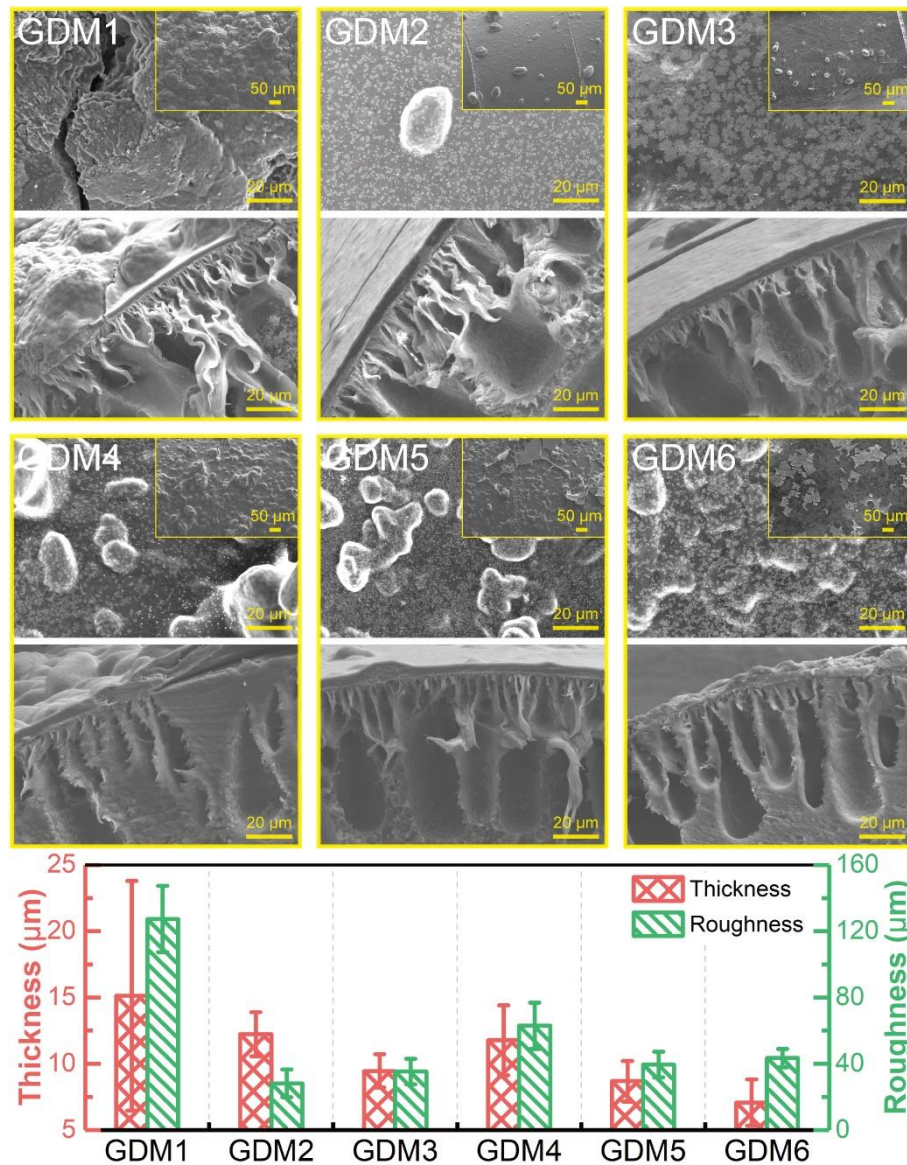
231 To summarize, pre-ozonation produced improved productivity in GDM filtration  
232 systems, which in fact increased as a function of ozonation strength. Smaller and  
233 more biodegradable organic compounds in the oxidized effluent would translate into a  
234 somewhat facilitated passage of organics into the permeate stream, also exacerbated  
235 by faster solubilization within the fouling layer. When adsorption of the oxidized  
236 effluent was included as an intermediate pre-treatment step, a higher removal rate of  
237 organics was consistently obtained compared to the treatment of the raw effluent  
238 without pre-ozonation. As suggested by these results, different properties and a

239 different composition of the membrane fouling layers should be expected following  
240 the different pre-treatment combinations, as fouling layers are a direct consequence of  
241 feed stream characteristics and water flux values.

### 242 **3.2 Characteristics of membrane fouling layers**

243 [Fig. S4](#), [Fig. S5](#), and [Fig. 2](#) present surface and cross-sectional micrographs of  
244 fouled membrane samples collected from the six GDM systems. A dense fouling layer  
245 was always observed, also corroborated by the fact that the typical IR peaks of virgin  
246 PVDF membrane disappeared in the FTIR spectra of fouled membranes ([Fig. S6c](#)).  
247 The layer thickness and roughness were the largest for the control GDM unit, while  
248 the distribution on the surface was very uneven. In addition, some pollutants were  
249 also deposited within the membrane pores. Compared with GDM and GGDM, the  
250 fouling layers of O<sub>3</sub>-GDM systems were consistently thinner.

251 As summarized in [Fig. S6a](#), the membrane fouling resistance of GDM systems is  
252 mainly reversible, with reversibility accounting for above 90% of the total resistance  
253 value. The pure water contact angles of fouling layers ([Fig. S6b](#)) indicated that  
254 pre-ozonation increased the hydrophilicity of the fouling layers by increasing the  
255 hydrophilicity of pollutants, while simultaneously GAC adsorption decreased the  
256 hydrophilicity of the fouling layers by absorbing hydrophilic pollutants.



257

258 **Fig. 2** Surface (top; 500 × and 100 ×) and cross-sectional (bottom; 500 ×) micrographs

259 of the fouled membrane samples from the six GDM systems, as well as thickness and

260 roughness values measured for the membrane fouling layers. GDM1, GDM2, GDM3,

261 GDM4, GDM5, and GDM6 represent control GDM, GGDM, O<sub>3</sub><sup>20</sup>-GGDM,

262 O<sub>3</sub><sup>40</sup>-GDM, O<sub>3</sub><sup>40</sup>-GGDM, and O<sub>3</sub><sup>80</sup>-GGDM units, respectively.

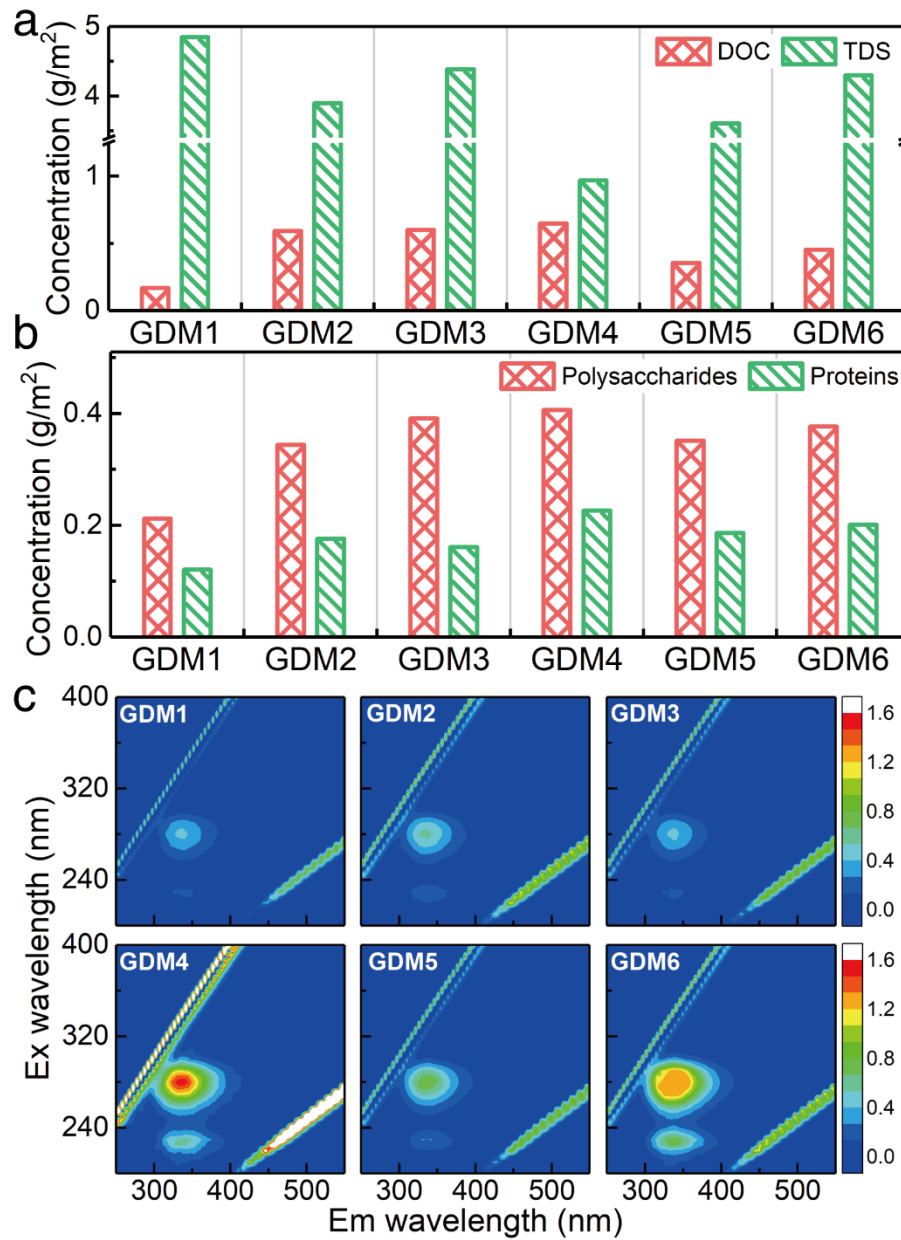
263

264 The results presented in **Fig. 3a** suggest that the accumulation of overall organic

265 contaminants on the membrane of control GDM and O<sub>3</sub><sup>40</sup>-GDM systems was the

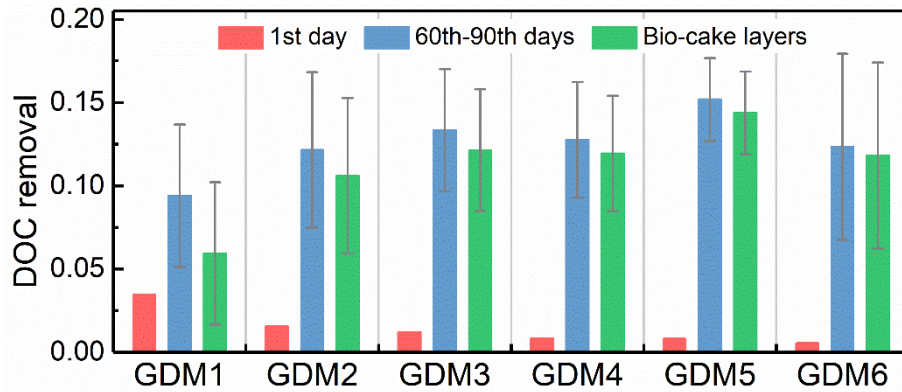


266 lowest and the largest, respectively. This observation is corroborated by the amount of  
267 EPS detected on the membranes and by the EEM analysis (Fig. 3b, c). The EPS  
268 content of the fouling layer in the four O<sub>3</sub>-GDM systems was higher than that  
269 observed in GDM and GGDM units, and highest in the O<sub>3</sub><sup>40</sup>-GDM unit. The same  
270 conclusion can be also drawn for fluorescent organic compounds. In particular, these  
271 compounds were distributed in region II (aromatic protein) and especially in region  
272 IV (soluble microbial by-product-like matters), suggesting the important contribution  
273 of transformation phenomena occurring within the fouling layer.



274

275 **Fig. 3** Concentration of (a) DOC and TDS, (b) EPS (includes polysaccharides and  
 276 proteins) in the fouling layers. (c) EEM spectra of compounds in the fouling layers.  
 277 GDM1, GDM2, GDM3, GDM4, GDM5, and GDM6 represent control GDM, GGDM,  
 278 O<sub>3</sub><sup>20</sup>-GGDM, O<sub>3</sub><sup>40</sup>-GDM, O<sub>3</sub><sup>40</sup>-GGDM, and O<sub>3</sub><sup>80</sup>-GGDM units, respectively.



279

280 Fig. 4 DOC removal of UF membrane of six GDM systems at 1st day and 60th-90th  
 281 days of operation and DOC removal of fouling layers at 60th-90th days. GDM1,  
 282 GDM2, GDM3, GDM4, GDM5, and GDM6 represent control GDM, GGDM,  
 283  $O_3^{20}$ -GGDM,  $O_3^{40}$ -GDM,  $O_3^{40}$ -GGDM, and  $O_3^{80}$ -GGDM, respectively.

284

285 The relative DOC removal rates of UF membranes can be obtained from the  
 286 varying concentrations of DOC in the reactor and effluent at any time to understand  
 287 the role of fouling layers as they form during operation (Fig. 4). The fouling layers  
 288 perform three functions, namely., physical interception, adsorption, and  
 289 biodegradation, which increase the contaminants removal in GDM systems (Tang et  
 290 al., 2021d). Specifically, the DOC removal attributable to the fouling layer can be  
 291 estimated by subtracting the DOC removal of the 1st day (no fouling layer present)  
 292 from that observed during the stable flux stage (days 60-90) . The DOC removal of  
 293 the fouling layer was 5.9% and 10.6% in control GDM and GGDM systems,  
 294 respectively. This parameter was significantly higher in all units treating pre-ozonized  
 295 streams. As mentioned above, the thickness of the fouling layer of GDM and GGDM

296 was thick and one would expect higher DOC removal by physical exclusion.  
297 Therefore, the higher DOC removal assessed in the four O<sub>3</sub>-GDM systems might be  
298 attributed to the higher biodegradation function of the fouling layers. In our work, we  
299 did not directly appraised the relative proportion of physical interception and  
300 biodegradation mechanisms resulting in organic removal. However, previous research  
301 indirectly determined the importance of these phenomena by adding biological  
302 inhibitors, such as sodium azide (Tang et al., 2021d), with results consistent with the  
303 present observations.

### 304 **3.3 Microbial diversity analysis**

305 The number of effective sequences, alpha diversity indexes, OUTs, and  
306 rarefaction curves for microbial communities in the raw water and in the fouling layer  
307 of the six GDM systems are presented in [Table 3](#) and [Fig.S7](#). The richness and  
308 diversity of microbial communities in the raw water were higher than those on  
309 membranes. The coverage values and rarefaction curves suggested the sequencing  
310 depth were sufficient.

311 Principal component analysis (PCA) at OUT level ([Fig. S8](#)) provides information  
312 on the affinity relationships of microbial community between the raw water and the  
313 fouling layers in the six GDM systems, as well as among the six GDM systems. The  
314 microbial community composition in the raw water was vastly different from that  
315 observed in the samples from the six GDM systems, indicating new dominant  
316 microorganisms had been formed in the filtration reactors. Also, pre-ozonation

317 seemed to have a large effect in the microbial community. The microbial community  
 318 compositions from the four GDM systems treating pre-ozonized SGW as feed water  
 319 were all similar, but different from the composition of the other two GDM systems  
 320 This result also indicates that GAC had little effect on the microbial community.

321

322 **Table 3** Number of effective sequences, OTUs, alpha diversity indexes for microbial  
 323 communities in the raw water and on the membrane of the six GDM systems.

Sample Name	Number of effective Sequences	OTUs at 97% identity	Shannon	Chao	Coverage
Raw water	36178	316	3.83	334.6	0.9988
GDM1	36064	115	2.50	119.2	0.9996
GDM2	30672	113	2.68	121.3	0.9994
GDM3	28903	88	2.52	107.4	0.9993
GDM4	29351	62	2.75	66.2	0.9997
GDM5	29713	92	2.93	105.0	0.9994
GDM6	24814	81	3.01	84.0	0.9997

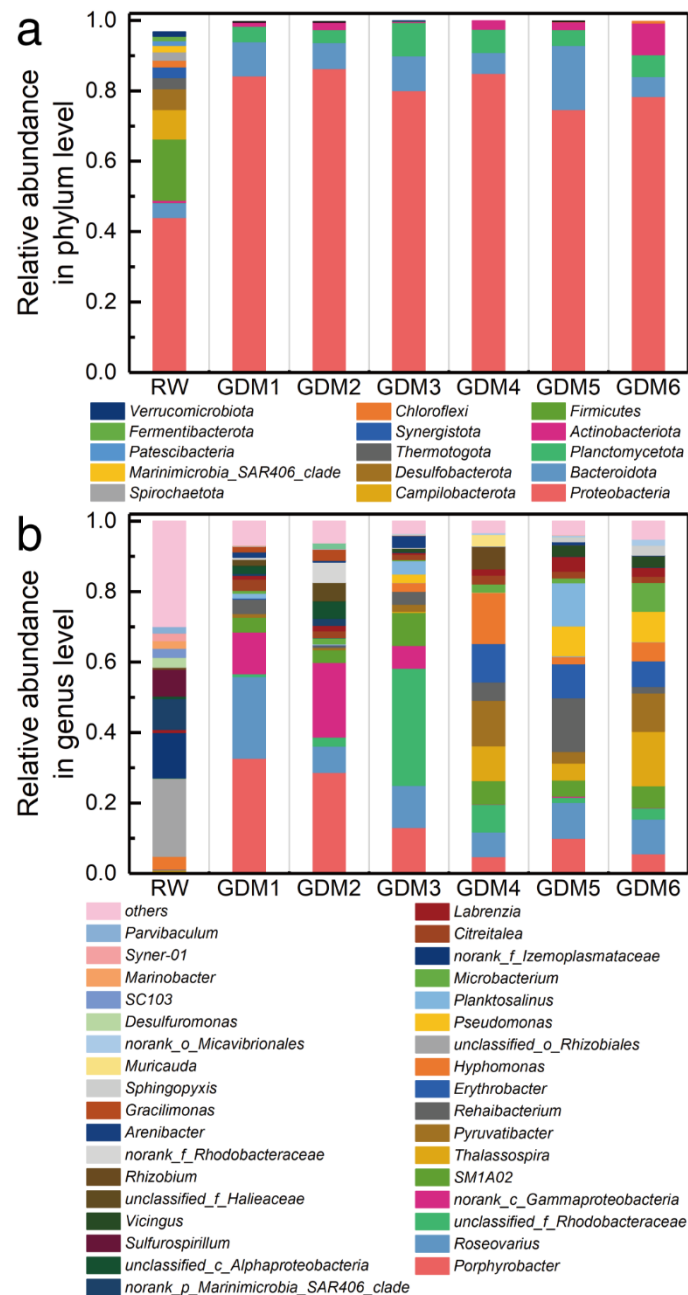
324

325 **Fig. 5a** and **Fig. 5b** show the microbial community composition at the phylum  
 326 and genus level, respectively. *Proteobacteria* (44.1%), *Firmicutes* (17.5%),  
 327 *Campilobacterota* (8.4%), *Desulfobacterota* (5.9%), and *Bacteroidota* (4.2%) were  
 328 the major phyla in the raw water, comprising 80.1% of bacteria. After operation,  
 329 *Proteobacteria* (74.8%-86.5%) and *Bacteroidota* (5.6%-18.2%) became the absolute  
 330 dominant microbial phyla in GDM reactors. The major genera in the raw water were  
 331 *unclassified\_o\_Rhizobiales*, *norank\_f\_Izemoplasmataceae*, *Parvibaculum*,

332 *Sulfurospirillum*, and *Desulfuromonas*. A large amount of relatively low abundance  
333 microorganisms (<0.5%) was enriched in GDM systems, like *Porphyrobacter*  
334 (4.8-32.8%), *Roseovarius* (7.0-23.2%), *unclassified\_f\_Rhodobacteraceae* (0.8-33.3%),  
335 *SMIA02* (3.6%-9.4%), *Pyruvatibacter* (0.6%-13.0%) and *Rehaibacterium*  
336 (0.5-15.2%). Some research showed that members of *Porphyrobacter* can degrade  
337 organics, such as polycyclic aromatic hydrocarbons (Balázs et al., 2020; Fan et al.,  
338 2016). *Roseovarius*, as an iodine oxidation bacterium, can promote the formation of  
339 large amounts of iodinated organic compounds (Almaraz et al., 2020).  
340 *Rhodobacteraceae* were widely reported in various environments with ability of  
341 degrading organic matter and removing nitrogen (Chen et al., 2021; Ma et al., 2020).  
342 Some works proved that *Pyruvatibacter* as a halophilic bacterium can degrade  
343 acetoacetic acid and pyruvate (Wang et al., 2016). *Rehaibacterium* was reported as a  
344 thermotolerant, halophilic, and strictly aerobic bacterium with the function of  
345 degrading some organic compounds (Yu et al., 2013).

346 In this work, O<sub>3</sub>-GDM systems had their own characteristic microorganisms.  
347 Specifically, *Porphyrobacter* and *norank\_c\_Gammaproteobacteria*, were enriched in  
348 the two GDM systems treating non-ozonized SGW as feed water. *Thalassospira*  
349 (5.0-15.5%), *Pyruvatibacter* (3.2-13.0%), and *Erythrobacter* (7.2-10.9%) were  
350 enriched in three of the O<sub>3</sub>-GDM systems. It was reported that some species of  
351 *Thalassospira* can degrade quaternary ammonium compounds, which are often used  
352 as biocides in SGW (Acharya et al., 2020). *Pyruvatibacter* as an aerobic marine

353 bacterium can degrade some organics, such as pyruvate (Wang et al., 2016). As  
 354 aerobic phototrophs, *Erythrobacter* often exist in organic-rich environments, and can  
 355 degrade PAHs, one of the main organic pollutants in SGW (Butkovskiy et al., 2017;  
 356 Kahla et al., 2021).



357  
 358 **Fig. 5** Bacterial community compositions at (a) the phylum (> 1%) and (b) the genus  
 359 level (> 1.5%) in raw water and on the membrane of the six GDM systems. GDM1,

360 GDM2, GDM3, GDM4, GDM5, and GDM6 represent control GDM, GGDM,  
361  $O_3^{20}$ -GGDM,  $O_3^{40}$ -GDM,  $O_3^{40}$ -GGDM, and  $O_3^{80}$ -GGDM units, respectively.

362

### 363 **3.4 Summary on mechanisms and effect of pre-ozonation on GDM systems and** 364 **desalination**

365 The rapid decline of flux in GDM system should be attributed to the blocking of  
366 membrane pores by the rapid formation of dense fouling layer (Fig. 1 and Fig. 2).  
367 Pre-ozonation significantly increased the initial flux (245%) but deteriorated the  
368 quality of effluent water in terms of DOC concentration (-14%) (Fig. 1). These results  
369 are mainly attributed to the conversion of macromolecular organics to low fractions  
370 by pre-ozonation (Fig. 1 and Fig. 4). EPS played an important role in flux  
371 development of GDM, and a large number of studies found negative correlation  
372 between EPS content and stable flux (Pronk et al., 2019; Tang et al., 2021d). However,  
373 some contradictory results were observed in this study.  $O_3$ -GDM system had higher  
374 EPS concentration compared to GDM (Fig. 3), while the stable flux of  $O_3$ -GDM  
375 system was 3.7 times of GDM. This observation suggests that there were other factors  
376 that played roles in stabilizing the flux. Compared with GDM, it was observed that the  
377 thickness of the fouling layer of  $O_3$ -GDM system was thinner, the hydrophilicity of  
378 the fouling layer was higher, and biodegradation ability of the fouling layer was  
379 enhanced (Fig. 2, Fig. S6, and Fig. 4). All these factors might play a positive function  
380 in the improvement of stable flux. However, we hypothesize that the reduction of

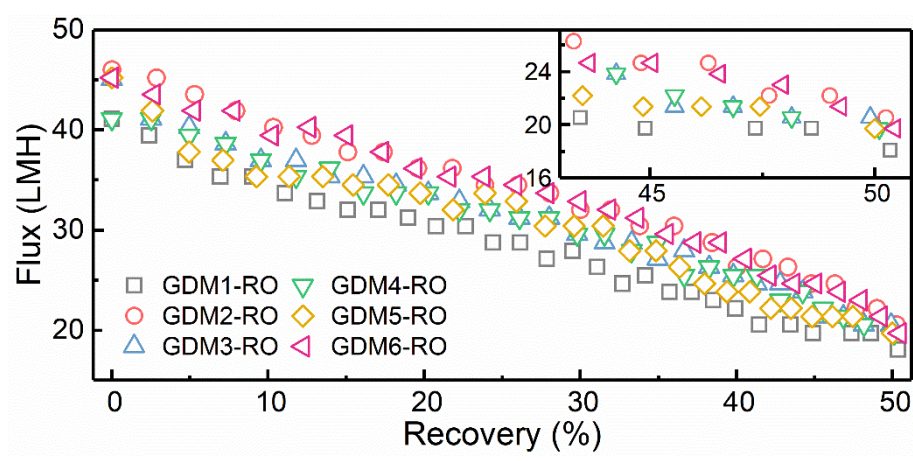


381 organics molecular size may be the main result of pre-ozonation that increased the  
382 stable flux.

383 Compared with GDM, GGDM had higher stable flux (637%), likely because  
384 GAC adsorption reduced the concentration of organic matters blocking membrane  
385 pores. For GGDM systems, pre-ozonation also markedly increased the flux (198%) in  
386 the first month of operation. Pre-ozonation improved the stable flux by reducing  
387 organics molecular size and GAC adsorption improved the stable flux by reducing the  
388 concentration of organic matters blocking membrane pores, also simultaneously  
389 improving the quality of the effluent.

390 The permeate of the six GDM systems was collected and fed individually to the  
391 RO system to study the effect of pretreatment on RO performance. The RO flux was  
392 higher when treating effluents that were previously ozonized, despite the fact the the  
393 DOC level in these streams was not necessarily lower than that from the control  
394 system ([Fig. 6](#)). Considering that the RO unit was operating in dead-end mode, the  
395 observed increase (9%) can be considered significant (Chang et al., 2019a). Some  
396 research found that pre-ozonation reduced RO membrane fouling by improving the  
397 hydrophilicity of foulants and weakening the adhesion forces between foulants and  
398 the membrane and among foulants (Yin et al., 2020a,b). Furthermore, the use of GAC  
399 significantly increased the flux of GDM-RO (13.6%) and slightly improve the flux of  
400 O<sub>3</sub>-GDM-RO. GAC adsorption may further reduce RO membrane fouling by  
401 decreasing the overall content of organic foulants (Monnot et al., 2017). [Table S1](#)

402 presents the effluent quality of six GDM-RO systems and indicates that within the  
 403 range of errors, the water quality of the six systems was almost the same. In general,  
 404 O<sub>3</sub>-GDM outperformed GDM in terms of productivity.



405  
 406 **Fig. 6** Effect of pretreatments on the RO desalination performance. GDM1, GDM2,  
 407 GDM3, GDM4, GDM5, and GDM6 represent control GDM, GGDM, O<sub>3</sub><sup>20</sup>-GGDM,  
 408 O<sub>3</sub><sup>40</sup>-GDM, O<sub>3</sub><sup>40</sup>-GGDM, and O<sub>3</sub><sup>80</sup>-GGDM units, respectively.

409  
 410 **4. Conclusions**

411 Pre-ozonation was investigated in combination with GAC adsorption and with  
 412 GDM system to treat SGW. Pre-ozonation changed the properties and molecular  
 413 weight of organic compounds. Macromolecular organics are oxidized by ozonation to  
 414 low fractions organics, which have a lower fouling tendency, can more easily pass  
 415 through the membrane pores, and can be more readily biodegraded the the  
 416 microorganisms in the fouling layers. At the same time, the decrease of the molecular  
 417 weight of organic matter also led to the deterioration of the effluent quality of  
 418 O<sub>3</sub>-GDM in terms of organic content. The higher concentration of organic compounds

419 in the feed solution and the laerger amount of EPS in the fouling layers of O<sub>3</sub>-GDM  
420 systems may be the reason why the stable flux of the systems treating ozonized  
421 effluents without adsorption was lower than that of systems including GAC. A large  
422 number of microorganisms with the ability to degrade organics and of denitrification  
423 were generally enriched in the membrane fouling layer. The O<sub>3</sub>-GDM systems had  
424 distinct core microorganisms that may help degrade characteristic organic compounds  
425 in SGW, such as quaternary ammonium compounds and PAHs. The contribution of  
426 microorganisms in the degradation of organic matter needs further investigation.

#### 427 **Supporting Information**

428 The Supporting Information is available free of charge on the website.

#### 429 **Acknowledgments**

430 This work was supported by the National Natural Science Foundation of China  
431 (52070134, 51678377), Xinglin Environment Project (2020CDYB-H02), and Sichuan  
432 University and Yibin City People's Government strategic cooperation project  
433 (2019CDYB-25). Thanks to the SEM measurement of the Institute of New Energy  
434 and Low-Carbon Technology, Sichuan University.

435 **References**

- 436 Acharya, S.M., Chakraborty, R. and Tringe, S.G. 2020. Emerging Trends in  
437 Biological Treatment of Wastewater From Unconventional Oil and Gas Extraction.  
438 *Front. Microbiol.* 11(2203). 10.3389/fmicb.2020.569019
- 439 Almaraz, N., Regnery, J., Vanzin, G.F., Riley, S.M., Ahoor, D.C. and Cath, T.Y.  
440 2020. Emergence and fate of volatile iodinated organic compounds during biological  
441 treatment of oil and gas produced water. *Sci. Total Environ.* 699, 134202.  
442 <https://doi.org/10.1016/j.scitotenv.2019.134202>
- 443 Balázs, H.E., Schmid, C.A.O., Podar, D., Hufnagel, G., Radl, V. and Schröder, P.  
444 2020. Development of microbial communities in organochlorine pesticide  
445 contaminated soil: A post-reclamation perspective. *Appl. Soil Ecol.* 150, 103467.  
446 <https://doi.org/10.1016/j.apsoil.2019.103467>
- 447 Butkovskiy, A., Bruning, H., Kools, S.A.E., Rijnaarts, H.H.M. and Van Wezel,  
448 A.P. 2017. Organic pollutants in shale gas flowback and produced waters: Identification,  
449 potential ecological impact, and implications for treatment strategies. *Environ. Sci.*  
450 *Technol.* 51(9), 4740-4754. <https://doi.org/10.1021/acs.est.6b05640>
- 451 Chang, H., Liu, B., Wang, H., Zhang, S.Y., Chen, S., Tiraferri, A. and Tang, Y.Q.  
452 2019a. Evaluating the performance of gravity-driven membrane filtration as  
453 desalination pretreatment of shale gas flowback and produced water. *J. Membr. Sci.*  
454 587, 117187. <https://doi.org/10.1016/j.memsci.2019.117187>
- 455 Chang, H., Liu, B., Yang, B., Yang, X., Guo, C., He, Q., Liang, S., Chen, S. and  
456 Yang, P. 2019b. An integrated coagulation-ultrafiltration-nanofiltration process for  
457 internal reuse of shale gas flowback and produced water. *Sep. Purif. Technol.* 211,  
458 310-321. <https://doi.org/10.1016/j.seppur.2018.09.081>
- 459 Chen, Z., Chang, Z., Qiao, L., Wang, J., Yang, L., Liu, Y., Song, X. and Li, J. 2021.  
460 Nitrogen removal performance and microbial diversity of bioreactor packed with  
461 cellulosic carriers in recirculating aquaculture system. *International Biodeterioration &*  
462 *Biodegradation* 157, 105157. <https://doi.org/10.1016/j.ibiod.2020.105157>
- 463 Ding, A., Liang, H., Li, G., Derlon, N., Szivak, I., Morgenroth, E. and Pronk, W.  
464 2016. Impact of aeration shear stress on permeate flux and fouling layer properties in a  
465 low pressure membrane bioreactor for the treatment of grey water. *J. Membr. Sci.* 510,  
466 382-390. <https://doi.org/10.1016/j.memsci.2016.03.025>
- 467 Fan, M., Lin, Y., Huo, H., Liu, Y., Zhao, L., Wang, E., Chen, W. and Wei, G. 2016.  
468 Microbial communities in riparian soils of a settling pond for mine drainage treatment.  
469 *Water Res.* 96, 198-207. <https://doi.org/10.1016/j.watres.2016.03.061>
- 470 Guo, C., Chang, H., Liu, B., He, Q., Xiong, B., Kumar, M. and Zydney, A.L. 2018.  
471 A combined ultrafiltration–reverse osmosis process for external reuse of Weiyuan shale  
472 gas flowback and produced water. *Environ. Sci. Water Res. Technol.* 4(7), 942-955.  
473 <https://doi.org/10.1039/C8EW00036K>
- 474 Kahla, O., Melliti Ben Garali, S., Karray, F., Ben Abdallah, M., Kallel, N., Mhiri,  
475 N., Zaghden, H., Barhoumi, B., Pringault, O., Quéméneur, M., Tedetti, M., Sayadi, S.

476 and Sakka Hlaili, A. 2021. Efficiency of benthic diatom-associated bacteria in the  
477 removal of benzo(a)pyrene and fluoranthene. *Sci. Total Environ.* 751, 141399.  
478 <https://doi.org/10.1016/j.scitotenv.2020.141399>

479 Kondash, A. and Vengosh, A. 2015. Water footprint of hydraulic fracturing.  
480 *Environ. Sci. Technol. Lett.* 2, 276–280. 10.1021/acs.estlett.5b00211

481 Lee, S., Badoux, G.O., Wu, B. and Chong, T.H. 2021. Enhancing performance of  
482 biocarriers facilitated gravity-driven membrane (GDM) reactor for decentralized  
483 wastewater treatment: Effect of internal recirculation and membrane packing density.  
484 *Sci. Total Environ.* 762, 144104. <https://doi.org/10.1016/j.scitotenv.2020.144104>

485 Liu, P., Ren, Y., Ma, W., Ma, J. and Du, Y. 2018. Degradation of shale gas  
486 produced water by magnetic porous MFe<sub>2</sub>O<sub>4</sub> (M = Cu, Ni, Co and Zn) heterogeneous  
487 catalyzed ozone. *Chem. Eng. J.* 345, 98-106. <https://doi.org/10.1016/j.cej.2018.03.145>

488 Ma, K., Li, X., Bao, L., Li, X. and Cui, Y. 2020. The performance and bacterial  
489 community shifts in an anaerobic-aerobic process treating purified terephthalic acid  
490 wastewater under influent composition variations and ambient temperatures. *J. Clean.*  
491 *Prod.* 276, 124190. <https://doi.org/10.1016/j.jclepro.2020.124190>

492 Miller, D.J., Huang, X., Li, H., Kasemset, S., Lee, A., Agnihotri, D., Hayes, T.,  
493 Paul, D.R. and Freeman, B.D. 2013. Fouling-resistant membranes for the treatment of  
494 flowback water from hydraulic shale fracturing: A pilot study. *J. Membr. Sci.* 437,  
495 265-275. <https://doi.org/10.1016/j.memsci.2013.03.019>

496 Monnot, M., Nguyễn, H.T.K., Laborie, S. and Cabassud, C. 2017. Seawater  
497 reverse osmosis desalination plant at community-scale: Role of an innovative  
498 pretreatment on process performances and intensification. *Chemical Engineering and*  
499 *Processing: Process Intensification* 113, 42-55.  
500 <https://doi.org/10.1016/j.cep.2016.09.020>

501 Pronk, W., Ding, A., Morgenroth, E., Derlon, N., Desmond, P., Burkhardt, M., Wu,  
502 B. and Fane, A.G. 2019. Gravity-driven membrane filtration for water and wastewater  
503 treatment: A review. *Water Res.* 149, 553-565.  
504 <https://doi.org/10.1016/j.watres.2018.11.062>

505 Sathya, U., Keerthi, Nithya, M. and Balasubramanian, N. 2019. Evaluation of  
506 advanced oxidation processes (AOPs) integrated membrane bioreactor (MBR) for the  
507 real textile wastewater treatment. *J. Environ. Manag.* 246, 768-775.  
508 <https://doi.org/10.1016/j.jenvman.2019.06.039>

509 Shang, W., Tiraferri, A., He, Q., Li, N., Chang, H., Liu, C. and Liu, B. 2019. Reuse  
510 of shale gas flowback and produced water: Effects of coagulation and adsorption on  
511 ultrafiltration, reverse osmosis combined process. *Sci. Total Environ.* 689, 47-56.  
512 <https://doi.org/10.1016/j.scitotenv.2019.06.365>

513 Tang, P., Li, J., Li, T., Tian, L., Sun, Y., Xie, W., He, Q., Chang, H., Tiraferri, A.  
514 and Liu, B. 2021a. Efficient integrated module of gravity driven membrane filtration,  
515 solar aeration and GAC adsorption for pretreatment of shale gas wastewater. *J. Hazard.*  
516 *Mater.* 405, 124166. <https://doi.org/10.1016/j.jhazmat.2020.124166>

517 Tang, P., Liu, B., Zhang, Y., Chang, H., Zhou, P., Feng, M. and Sharma, V.K. 2020.

518 Sustainable reuse of shale gas wastewater by pre-ozonation with ultrafiltration-reverse  
519 osmosis. Chem. Eng. J. 392, 123743. <https://doi.org/10.1016/j.cej.2019.123743>  
520 Tang, P., Xie, W., Tiraferri, A., Zhang, Y., Zhu, J., Li, J., Lin, D., Crittenden, J.C.  
521 and Liu, B. 2021b. Organics removal from shale gas wastewater by pre-oxidation  
522 combined with biologically active filtration. Water Res. 196, 117041.  
523 <https://doi.org/10.1016/j.watres.2021.117041>  
524 Tang, X., Pronk, W., Traber, J., Liang, H., Li, G. and Morgenroth, E. 2021c.  
525 Integrating granular activated carbon (GAC) to gravity-driven membrane (GDM) to  
526 improve its flux stabilization: Respective roles of adsorption and biodegradation by  
527 GAC. Sci. Total Environ. 768, 144758. <https://doi.org/10.1016/j.scitotenv.2020.144758>  
528 Tang, X., Zhu, X., Huang, K., Wang, J., Guo, Y., Xie, B., Li, G. and Liang, H.  
529 2021d. Can ultrafiltration singly treat the iron- and manganese-containing groundwater?  
530 J. Hazard. Mater. 409, 124983. <https://doi.org/10.1016/j.jhazmat.2020.124983>  
531 Tong, T., Carlson, K.H., Robbins, C.A., Zhang, Z. and Du, X. 2019.  
532 Membrane-based treatment of shale oil and gas wastewater: The current state of  
533 knowledge. Front. Env. Sci. Eng. 13(4), 63.  
534 <https://doi.org/10.1016/j.watres.2020.115694>  
535 Wang, G., Tang, M., Wu, H., Dai, S., Li, T., Chen, C., He, H., Fan, J., Xiang, W.  
536 and Li, X. 2016. *Pyruvatibacter mobilis* gen. nov., sp. nov., a marine bacterium from the  
537 culture broth of *Picochlorum* sp. 122. 66(1), 184-188.  
538 <https://doi.org/10.1099/ijsem.0.000692>  
539 Wang, H., Park, M., Liang, H., Wu, S., Lopez, I.J., Ji, W., Li, G. and Snyder, S.A.  
540 2017. Reducing ultrafiltration membrane fouling during potable water reuse using  
541 pre-ozonation. Water Res. 125, 42-51. 10.1016/j.watres.2017.08.030  
542 Yin, Z., Wen, T., Li, Y., Li, A. and Long, C. 2020a. Alleviating reverse osmosis  
543 membrane fouling caused by biopolymers using pre-ozonation. J. Membr. Sci. 595,  
544 117546. <https://doi.org/10.1016/j.memsci.2019.117546>  
545 Yin, Z., Wen, T., Li, Y., Li, A. and Long, C. 2020b. Pre-ozonation for the  
546 mitigation of reverse osmosis (RO) membrane fouling by biopolymer: The roles of  
547  $\text{Ca}^{2+}$  and  $\text{Mg}^{2+}$ . Water Res. 171, 115437. <https://doi.org/10.1016/j.watres.2019.115437>  
548 Yu, T.-T., Yao, J.-C., Yin, Y.-R., Dong, L., Liu, R.-F., Ming, H., Zhou, E.-M. and  
549 Li, W.-J. 2013. *Rehaibacterium terrae* gen. nova, sp nov isolated from a geothermally  
550 heated soil sample. Int. J. Syst. Evol. Micr. 63, 4058-4063. 10.1099/ijss.0.049973-0  
551 Zhang, K., Zhang, Z.-h., Wang, H., Wang, X.-m., Zhang, X.-h. and Xie, Y.F. 2020.  
552 Synergistic effects of combining ozonation, ceramic membrane filtration and  
553 biologically active carbon filtration for wastewater reclamation. J. Hazard. Mater. 382,  
554 121091. <https://doi.org/10.1016/j.jhazmat.2019.121091>  
555